This document was prepared for the ETI by third parties under contract to the ETI. The ETI is making these documents and data available to the public to inform the debate on low carbon energy innovation and deployment.

Programme Area: Marine

Project: PerAWAT

Title: Report on Assessment of the Impact of Energy Extraction for the Horizontal Axis Tidal Turbine on Large Scale Tidal Characteristics at Example UK Sites

Abstract:

This deliverable focuses on the large-scale changes to the tidal hydrodynamics from the extraction of energy using tidal stream turbines. Large scale in this context means at larger scales than the wake behind an individual tidal turbine. The sites studied in this project are Pentland Firth, Anglesey and Bristol Channel. The report concludes that there are near field impacts (turbines cause reduction in flow), but no far field impacts (say between Anglesey and Bristol Channel). Environmental impact is outside the scope of the report.

Context:

The Performance Assessment of Wave and Tidal Array Systems (PerAWaT) project, launched in October 2009 with £8m of ETI investment. The project delivered validated, commercial software tools capable of significantly reducing the levels of uncertainty associated with predicting the energy yield of major wave and tidal stream energy arrays. It also produced information that will help reduce commercial risk of future large scale wave and tidal array developments.

Energy Technologies Institute

PerAWaT

WG3 WP6 D8 — REPORT ON ASSESSMENT OF THE IMPACT OF ENERGY EXTRACTION FOR THE HORIZONTAL AXIS TIDAL TURBINE ON LARGE SCALE TIDAL CHARACTERISTICS AT EXAMPLE UK SITES

Authors S. Serhadlıoğlu, T.A.A. Adcock,
G.T. Houlsby, and A.G.L. Borthwick

Version 1.0

Date 09/12/2013

Revision History		
Issue / Version	Issue Date	Summary
0.0	05/11/2013	Draft of the report submitted to GH.
1.0	09/12/2013	Report submitted to ETI.

Executive Summary

WG3 WP6 D8 focuses on the large-scale changes to the tidal hydrodynamics from the extraction of energy using tidal stream turbines. Large scale in this context means at larger scales than the wake behind an individual tidal turbine.

There will clearly be a significant local impact on the hydrodynamics close to the tidal turbine as flow is accelerated around the turbines. There will also be an increase in turbulence intensity due to the turbines. These may impact on the local wildlife and cause significant localised changes to the sediment transport in the region of the turbines. However, these changes are beyond the scope of this work package.

The basin-scale models used in this work package are used to examine (a) the influence of the location of turbine arrays on the power output, (b) the changes to the local hydrodynamics due to the placement of the arrays and (c) interactions between arrays placed in multiple locations.

This report analyses these changes for the three sites studied in this project (Pentland Firth, Anglesey and Bristol Channel) and introduces a general analytical model for describing these changes at all sites.

CONTENTS

1. Introduction

Acceptance Criteria

Table 1 lists the acceptance criteria for the present deliverable.

Deliverable
WG3 WP6 D8: Report on assessment of the impact of energy extraction for the horizontal axis tidal turbine on large scale tidal characteristics at example UK sites
Acceptance Criteria
Report describes: - the methodology for assessing the impact of energy extraction at different sites, - an assessment of the effect of energy extraction for the horizontal axis turbine at the different sites, - discussion of the model performance, including review of applications, sensitivities and limitations.

Table 1 Acceptance criteria.

Methodology

Two approaches are used in this report: 2D depth-integrated numerical modelling and semi-analytical modelling.

The 2D depth-integrated model developed as part of this work package has been documented in various deliverables — particularly WG3 WP6 D5. A brief description is included here. The numerical model used in this work package is the discontinuous Galerkin (DG) ADCIRC model, developed by Kubatko *et al*. (2006 and 2009). The presence of tidal turbines is included in this model through a line-sink of momentum included by imposing a depth-change across the row of tidal turbines. The numerical implementation and theory for this are described in WG3 WP6 D5.

The semi-analytical modelling is an extension of the approach taken by Garrett and Cummins (2005). They modelled a tidal channel between two oceans whose water level was not modified by the dynamics within the channel. In this report we extend this to a channel split into sub-channels and produce an analytical model of the extractable power. This work has been accepted for publication (Draper, 2013a,b). The methodology is described in detail in Draper (2013b) included with this report. The environmental change has also been examined as part of an additional paper written as part of this project and included with this report (Adcock and Draper, 2014).

Sections 2 and 3 present the results obtained for turbine array deployment in the Anglesey headland region and the Bristol Channel respectively. Section 4 considers both sites together, the aim being to assess whether any significant hydrodynamic interactions could occur as a result of tidal farm deployments at both sites together. Section 5 presents results obtained for different tidal array deployments in the Pentland Firth. Finally, Section 6 presents the conclusions.

2. Anglesey

Description of the Model

WG3 WP6 D7 discusses that mapping the undisturbed kinetic energy flux within a site is a good indicator for selecting where the tidal turbine arrays are to be deployed. With this in mind, Figure 1 illustrates the map of the undisturbed kinetic energy flux density off the Anglesey site. It can be seen that there are several locations at Anglesey site, which are favourable for tidal array deployments. The sites that are chosen for analysing the tidal farm interactions are summarised in Table 2.

The analysis follows the same approach as taken in WG3 WP6 D7. Here, it is intended to examine the extent of the disturbance to the local hydrodynamics caused by the presence of the turbine arrays. In each simulation, the effect of the turbine array is represented using linear momentum actuator disk theory (Houlsby *et al.*, 2008) for a high blockage ratio ($B = 0.5$) and the computed optimum wake velocity

coefficient. Each simulation covers a full spring-neap cycle. The forcing harmonics are the dominant semidiurnal M_2 and S_2 tides. The model parameters include the Coriolis force and a constant eddy viscosity term of 3 kg/(s.m). The bed friction coefficient used in the simulations is $C_f = 0.0025$.

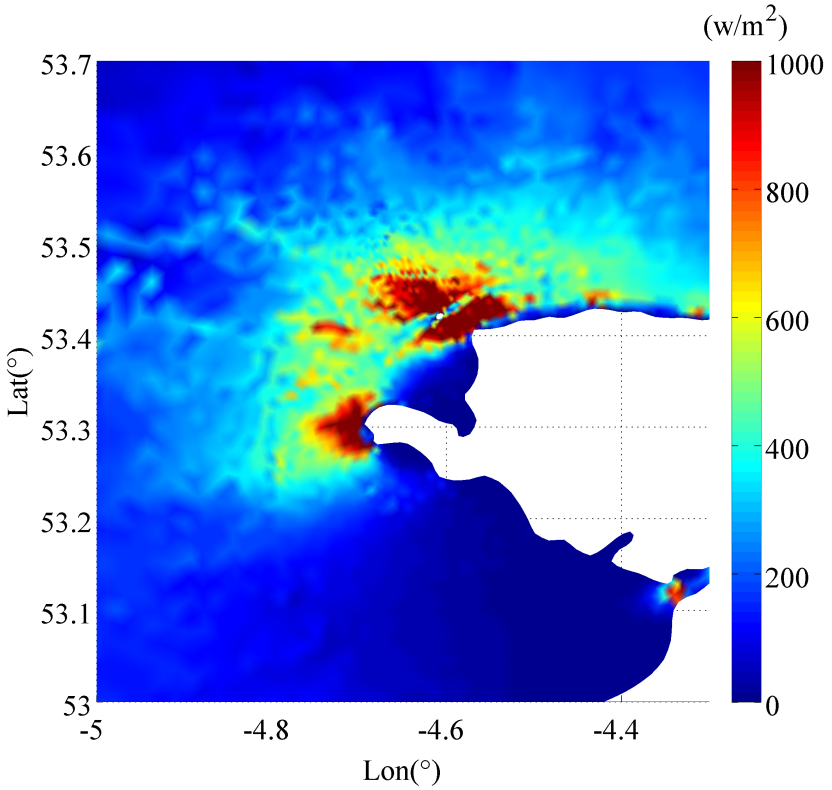

Figure 1 Undisturbed kinetic energy density map off Anglesey headland

Site	Location	Coordinates	Undisturbed kinetic energy flux density, ρ_{KE} (W/m^2)
Anglesey	Holyhead (HH)	53°18'10"N 4°45'58"W	720
	Skerries – Offshore (SO)	53°26'37"N 4°39'23"W	680
	Skerries - Strait (SS)	53°24'52"N 4°35'14"W	1460

Table 2 Locations where high tidal currents are observed off Anglesey site.

Analyses on Individual Array Deployments

WG3 WP6 D7 has introduced a parametric study focusing solely on tidal farm deployments near the Anglesey Skerries. The present section investigates potential interactions between tidal farm sites located in close vicinity to each other off the Anglesey headland.

Figure 2 illustrates the locations of the selected tidal farm sites. Following the methodology explained in WG3 WP6 D7, a parametric study has been conducted in order to compute the optimum wake velocity coefficient for a high blockage case. Using a fixed blockage ratio ($B = 0.5$) and varying the prescribed wake velocity coefficient (α_4), the optimum wake velocity coefficient is computed by fitting a spline to the averaged available power values obtained from each simulation.

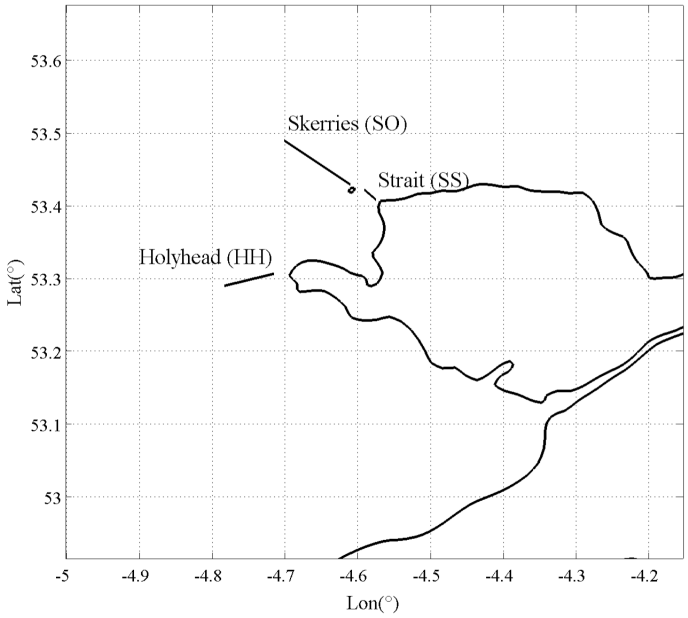

Figure 2 Locations of selected tidal farms off Anglesey headland

Table 3 summarises the computed optimum (α_4) values and the corresponding maximum available and extracted power values that are averaged over a tidal spring-neap cycle for each region considered.

Location	Length (km)	Optimum (α_4)	Maximum available power (MW)	Maximum extracted power (MW)
Holyhead (HH)	4.9	0.48	168.3	275.9
Skerries - Offshore (SO)	9.1	0.46	385.8	658.1
Skerries - Strait (SS)	1.8	0.55	86	127.7

Table 3 Optimum wake velocity coefficients of the arrays located at different sites off Anglesey. The maximum available and extracted power values are also given.

The change in the local hydrodynamics is estimated by considering only the semidiurnal M_2 and S_2 harmonics. Figure 3 shows selected stations where the changes in harmonic constituents are computed. Stations S1, S2 and S3 are chosen to evaluate changes to the far field owing to the energy extraction from the different sites, whereas S4 is selected to compare changes to the hydrodynamics near the coast of Anglesey headland. The remaining observation points are selected to examine the effects upstream and downstream of each individual tidal farm.

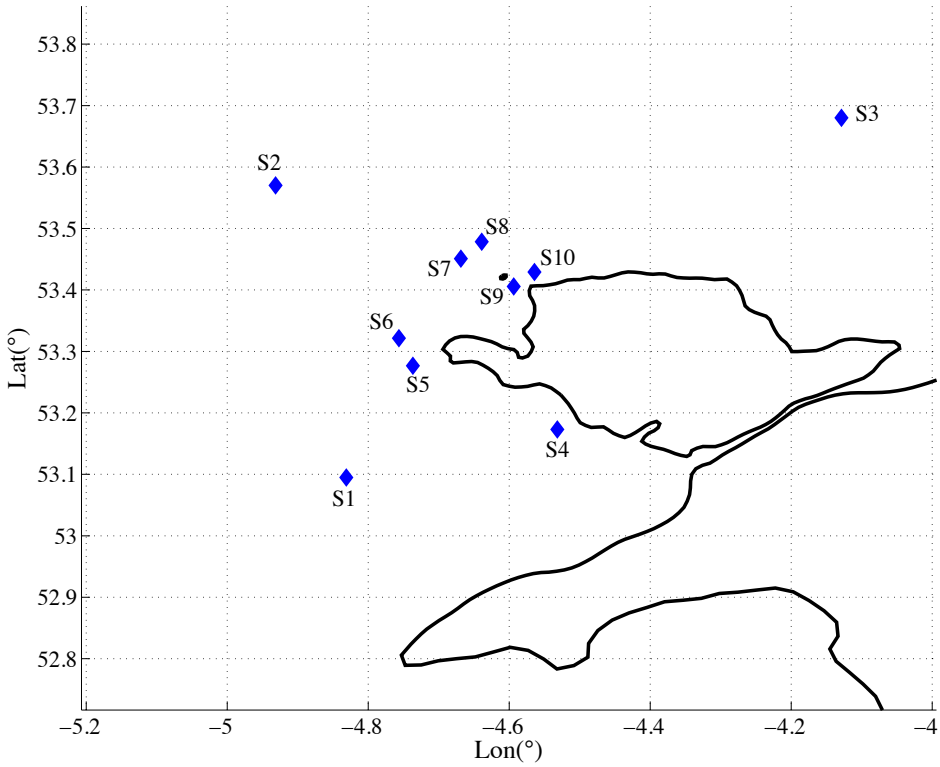

Figure 3 Locations of the stations off Anglesey, selected for comparison

Table 4 and Table 5 present the harmonic analysis of the tidal amplitude results for the M_2 and S_2 tidal constituents respectively. Table 4 shows that the M_2 amplitude changes in the vicinity of the arrays are within 1% for the Holyhead (HH) and Skerries-Strait (SS) cases. This change is slightly higher (2.5 – 3 %) for the Skerries-Offshore (SO) case owing to the higher thrust applied to the flow because of the length of the array. The M_2 phases do not alter significantly due to the presence of the arrays. The maximum change is observed in the Skerries-Offshore case, in which high water occurs approximately 5 min (~ 2.6°) earlier than natural upstream of the array, whereas it is delayed around 2 min at the downstream location. It should be noted that the upstream and downstream locations relative to the arrays are determined with respect to the direction of the flood tide.

Station	Amplitude (m)				Phase (°)			
	Natural	*HH*	*SO*	*SS*	*Natural*	*HH*	*SO*	*SS*
S1	1.44	1.44	1.48	1.44	284	283	283	284
S2	1.88	1.88	1.93	1.88	310	310	309	310
S3	2.54	2.54	2.58	2.54	319	320	319	320
S4	1.60	1.60	1.64	1.59	281	280	281	281
S5	1.70	1.71	1.74	1.70	290	289	289	290
S6	1.77	1.77	1.81	1.77	294	295	294	294
S7	2.02	2.03	2.07	2.03	303	304	301	303
S8	2.08	2.08	2.13	2.08	306	306	307	306
S9	2.04	2.04	2.08	2.03	300	300	299	299
S10	2.12	2.13	2.17	2.14	305	305	305	305

Table 4 Amplitude and phase of the M_2 tidal elevations at different observation stations off Anglesey under natural conditions and in the presence of different array configurations.

The change in the semidiurnal solar harmonic S_2, due to the presence of arrays, is insignificant. Table 5 summarises the predicted S_2 elevation amplitudes and phases at different observation stations. The amplitudes differ by approximately 0.01 m. Across the turbine arrays, the phases change by 5° at the Skerries-Offshore (SO) case. However, for other case studies the average difference is approximately 2°.

At a tidal array, the partially blocked flow tends to divert around the turbines, as discussed previously in WG3 WP6 D7. This in turn results in a decrease in the flow

through the array site, and an increase of the bypass flow.

Station	Amplitude (m)				Phase (°)			
	Natural	*HH*	*SO*	*SS*	*Natural*	*HH*	*SO*	*SS*
S1	0.52	0.52	0.53	0.52	313	313	313	313
S2	0.58	0.57	0.58	0.57	340	340	339	340
S3	0.73	0.72	0.73	0.72	354	355	354	355
S4	0.57	0.57	0.57	0.56	311	311	311	311
S5	0.57	0.58	0.58	0.57	320	318	319	320
S6	0.58	0.57	0.59	0.58	324	325	324	324
S7	0.63	0.63	0.64	0.63	334	335	331	334
S8	0.63	0.63	0.63	0.63	337	338	339	337
S9	0.63	0.63	0.63	0.63	331	331	331	330
S10	0.64	0.64	0.64	0.64	337	337	337	338

Table 5 Amplitude and phase of the S_2 tidal elevations at different observation stations off Anglesey under natural conditions and in the presence of different array configurations.

Table 6, Table 7, Table 8 and Table 9 present the change in the M_2 and S_2 tidal currents due to the presence of the individual tidal arrays. From Table 6, it can be seen that the M_2 tidal current magnitudes are not changed greatly at the offshore stations S1, S2 and S3. However, in the vicinity of the arrays, the velocity magnitudes decrease considerably. For the Holyhead (HH) array, the M_2 velocity magnitude decreases by 13% upstream and 9% on the downstream of the array. The estimated velocity magnitude changes for the Skerries-Offshore (SO) array is 16% upstream and 11% downstream. The maximum difference is observed for the Skerries-Strait (SS) array. The upstream M_2 velocity magnitude is altered by ~25% upstream and by ~20% downstream of the array.

The M_2 velocity phase lags show that for Skerries-Offshore (SO) and Holyhead (HH) arrays, fastest currents occur approximately 20 min earlier than natural case. This change is less significant at the Skerries-Strait (SS) array, where the currents reach their maximum speed 5 min earlier than the natural case. The Skerries-Offshore (SO) array affects the tides reaching the strait between Anglesey Skerries and the headland. From Table 6, the M_2 phase lag difference observed in the stations S9 and S10 indicate that the fastest currents are delayed. This delay is approximately 15 min

at the S9 station. However at S10, the fastest currents are delayed by 5 min.

Station	U_{mag} (m/s)				φ_{mag} (°)			
	Natural	*HH*	*SO*	*SS*	*Natural*	*HH*	*SO*	*SS*
S1	0.82	0.82	0.81	0.82	228	228	228	228
S2	0.96	0.97	0.98	0.97	239	240	241	240
S3	0.82	0.82	0.81	0.82	240	241	240	241
S4	0.39	0.38	0.40	0.39	229	226	229	230
S5	1.47	1.28	1.44	1.46	226	219	226	226
S6	1.28	1.16	1.22	1.26	227	217	225	227
S7	1.48	1.47	1.25	1.50	230	230	221	230
S8	1.47	1.47	1.31	1.49	232	232	223	232
S9	2.17	2.16	2.28	1.65	206	206	213	204
S10	2.02	2.01	2.05	1.60	217	217	219	214

Table 6 Amplitude and phase of the M_2 tidal current at different observation stations in the Irish Sea off Anglesey under natural conditions and in the presence of different array configurations.

Stations	Eccentricity				Inclination (°)			
	Natural	*HH*	*SO*	*SS*	*Natural*	*HH*	*SO*	*SS*
S1	0.097	0.124	0.098	0.098	83	84	83	83
S2	-0.101	-0.107	-0.091	-0.100	44	44	44	44
S3	-0.032	-0.031	-0.039	-0.033	3	3	2	3
S4	0.117	0.115	0.101	0.119	116	115	118	116
S5	0.038	0.011	0.037	0.037	105	106	105	105
S6	0.080	0.108	0.088	0.090	76	73	76	77
S7	-0.040	-0.059	-0.079	-0.048	38	37	39	38
S8	-0.030	-0.041	-0.013	-0.033	28	27	26	28
S9	-0.082	-0.083	-0.069	-0.099	51	51	51	54
S10	-0.001	-0.010	0.002	0.021	31	31	31	28

Table 7 Eccentricity and inclination of the M_2 currents at different observation stations in the Irish Sea off Anglesey under normal conditions and in the presence of different array configurations.

The eccentricity and inclination (Table 7) values indicate the impact on the "tidal ellipses" which express a rectilinear flow when eccentricity is equal to 0 and a circular flow when eccentricity is 1. For far-field observation stations, considering that the semi-major axis values do not change significantly, the observed change in eccentricity relates to the change in semi-minor axis. Noting the results obtained for

these far-field stations, it appears that the presence of HH array has an impact on the tidal ellipse structure in the incoming tide from the western Irish Sea. The presence of the Skerries-Offshore (SO) array has a similar effect on the tidal ellipse structure observed in the western Irish Sea. The case study concerning the operation of the Skerries-Strait (SS) array indicates that the ellipse structure is changing in the Anglesey Skerries offshore site as well as in the strait. This result implies that the change in the hydrodynamics is limited within the vicinity of the array and is influenced by the coastal characteristics of the site.

A similar analysis has been conducted for S_2 tidal currents. Table 8 shows the maximum current magnitudes and phase lags at different observation stations around the Irish Sea, which are computed for conditions when there is no array operating (Natural) and when there are arrays present (HH, SO and SS). The table shows that the far-field stations are not affected by the existence of the arrays. However, the current magnitudes decrease both upstream and downstream of the arrays. The change is about 20% at the HH and SO arrays, and 30% at the SS array. The reason for this considerable difference is primarily due to flow diversion. The phase lags indicate a maximum of 30 minutes delay for the S_2 tidal currents to reach their maximum at the vicinity of the arrays.

Station	U_{mag} (m/s)				φ_{mag} (°)			
	Natural	*HH*	*SO*	*SS*	*Natural*	*HH*	*SO*	*SS*
S1	0.24	0.24	0.24	0.24	264	264	264	264
S2	0.28	0.28	0.28	0.28	278	280	281	280
S3	0.25	0.24	0.24	0.24	280	280	279	280
S4	0.12	0.11	0.12	0.12	261	257	260	261
S5	0.48	0.36	0.47	0.47	259	251	257	259
S6	0.38	0.33	0.38	0.38	264	248	257	263
S7	0.45	0.44	0.35	0.45	266	266	254	266
S8	0.45	0.44	0.37	0.45	268	268	256	268
S9	0.61	0.60	0.60	0.41	234	232	242	231
S10	0.59	0.57	0.57	0.42	248	247	251	244

Table 8 Amplitude and phase of the S_2 tidal current at different observation stations in the Irish Sea off Anglesey under natural conditions and in the presence of different array configurations.

Table 9 lists the eccentricity and inclination values for S_2 tidal current ellipses. According to Table 9, the SS array mainly affects the region offshore of Anglesey Skerries (again due to the flow diversion). For station S8, the presence of arrays changes the direction of the S_2 tidal ellipse from anti-clockwise to clockwise.

Station	Eccentricity				Inclination (°)			
	Natural	*HH*	*SO*	*SS*	*Natural*	*HH*	*SO*	*SS*
S1	0.126	0.175	0.133	0.130	82	82	82	82
S2	-0.054	-0.069	-0.053	-0.060	42	42	43	42
S3	-0.030	-0.024	-0.039	-0.026	2	2	1	2
S4	0.161	0.125	0.146	0.166	115	115	116	114
S5	0.063	0.035	0.053	0.064	103	105	104	104
S6	0.112	0.164	0.106	0.119	79	73	78	80
S7	-0.019	-0.077	-0.071	-0.048	37	37	39	38
S8	0.006	-0.033	-0.003	-0.013	27	27	26	27
S9	-0.083	-0.093	-0.057	-0.119	47	48	48	52
S10	0.064	0.028	0.019	0.053	29	31	32	29

Table 9 Eccentricity and inclination of the S_2 currents at different observation stations in the Irish Sea off Anglesey under normal conditions and in the presence of different array configurations.

Analyses of Multiple Array Deployments

This subsection considers the effect of installing multiple arrays within the Anglesey basin. The array configurations studied in this section are:

1. Holyhead and Skerries-Offshore (HH + SO),
2. Holyhead and Skerries-Strait (HH + SS),
3. Skerries-Offshore and Skerries-Strait (SO + SS) and,
4. Holyhead, Skerries-Offshore and Skerries-Strait (HH + SO + SS).

Regarding the power that is available to the arrays, WG3 WP6 D7 previously concluded that arrays connected in parallel interact constructively, and those in series interact destructively. For a spring-neap cycle, a similar analysis has been conducted to evaluate the total available power from the site for each array configuration. The simulations use the optimum wake velocity coefficients presented in Table 3. The local blockage ratio is set to 0.5 and the model is forced with the dominant semi-diurnal tides M_2 and S_2. Table 10 shows the simulated available power output (P_{avail})

and the arithmetic sum of the available power outputs (ΣP_{avail}) for each array combination. From Table 10, it is evident that when Holyhead (HH) array is operating along with other arrays, there is no significant change in the power extracted by the either turbine array. However, operation of the Skerries-Offshore (SO) array together with the Skerries-Strait (SS) array corresponds to operating arrays connected in parallel, thus increasing the local blockage, which increases the available power. The arithmetic sum of the available power of SO and SS arrays that operate in isolation is 471.8 MW, whereas the simulated available power is 515.4 MW. There is a 44.2 MW (8.5%) increase of the available power in this configuration due to parallel operation. For Case Study 4, when all the arrays are operating together, the enhancement over the sum of the individual arrays is only 28.1 MW, as compared to the 44.2 MW increase when SS and SO are operated together. The decrement of 16.1 MW is attributed to the destructive interference of the HH array acting in series with the other two arrays. Interestingly, this decrement is significantly higher than that observed when combining HH + SO or HH + SS. This is attributed (qualitatively) to the fact that it is only when SS and SO are both operated that there is any effective barrier in series with HH.

Case Study	Array Combinations	P_{avail} (MW)	$\sum P_{avail}$ (MW)
1	HH + SO	553.3	554.1
2	HH + SS	254	254.3
3	SO + SS	515.4	471.8
4	HH + SO + SS	668.4	640.1

Table 10 Comparison of the estimated (P_{avail}) and calculated (ΣP_{avail}) available power output for each test case studied for Anglesey region.

The local hydrodynamics of the system is evaluated by focusing on the M_2 tidal harmonic constituent. The change in the M_2 elevation amplitudes is illustrated in Figure 4 for each case study.

Case 1 involves the Holyhead (HH) and Skerries-Offshore (SO) arrays. Figure 4(a)

shows that the M_2 tidal amplitudes are increased by an average of 1.5 cm at the upstream of the HH array (regarding the direction of the flood tide). This is expected as the tidal devices are acting as an additional resistance to the flow, which causes the flow to build up in front of the devices. Due to the energy extraction, there is a head drop observed across the array. The total head drop across the array is approximately 3 cm for the HH array. As for the SO array, the flow tends to divert towards the northern edge of the array. The diversion of the flow reduces the mass flux entering the array closer to the Skerries, thus reducing the M_2 tidal elevations over that region.

Figure 4(b) shows the M_2 elevation amplitude change for the Holyhead (HH) and Skerries-Strait (SS) arrays. The Holyhead (HH) array behaves in a similar manner as in Figure 4(a). For the SS array, it is evident that the amplitudes are decreased at the upstream side (regarding the direction of the flood tide) of the array due to the flow diversion. During the ebb tide, however, the amplitudes are increased in front of the array due to the additional resistance. The head drop across the SS array is approximately 2 cm in average. Figure 4(c) and Figure 4(d) reveal that the arrays act individually and do not interact significantly as far as M_2 elevation amplitudes are concerned. The arrays behave in a similar manner for each case study.

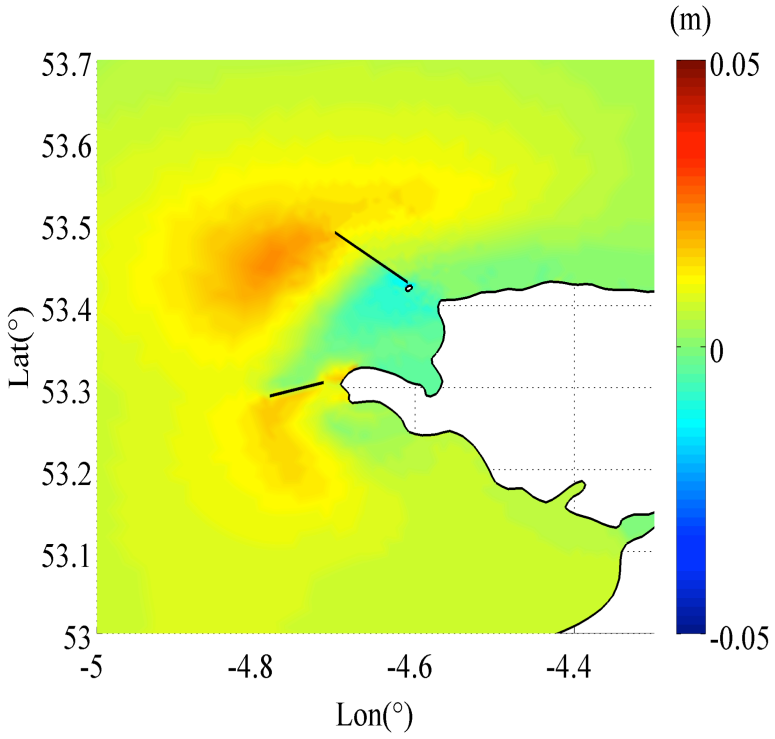

a) HH and SO arrays

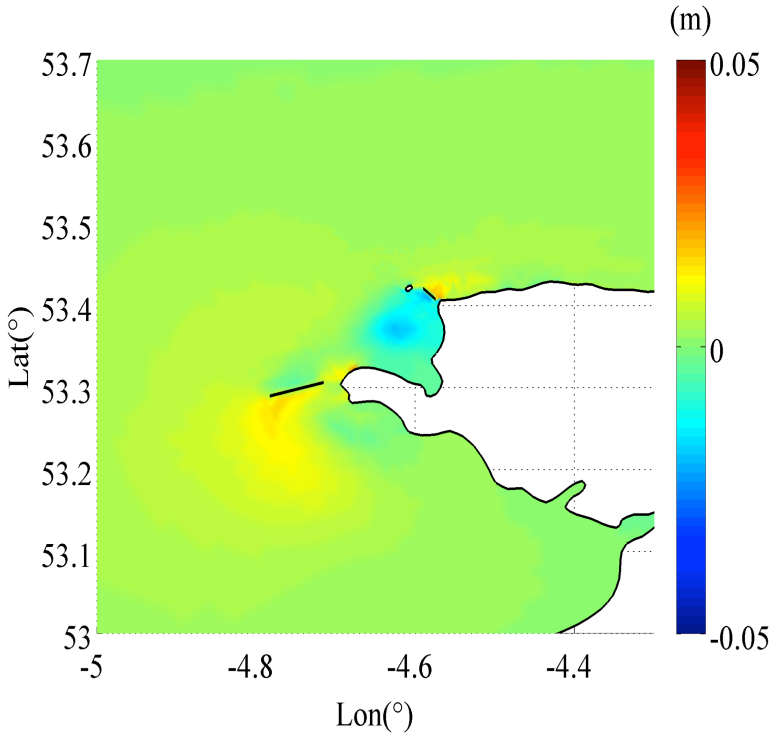

b) HH and SS arrays

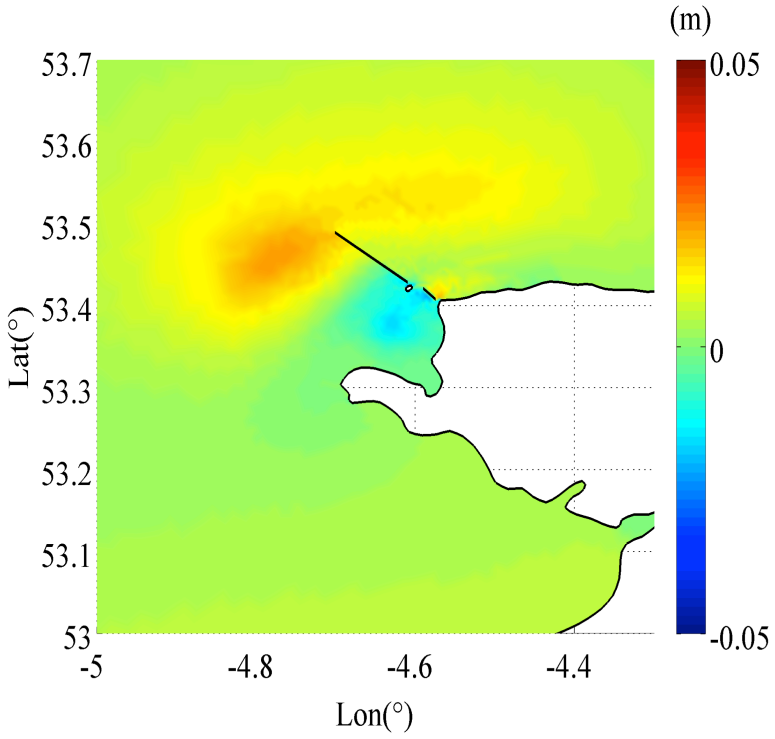

c) SO and SS arrays

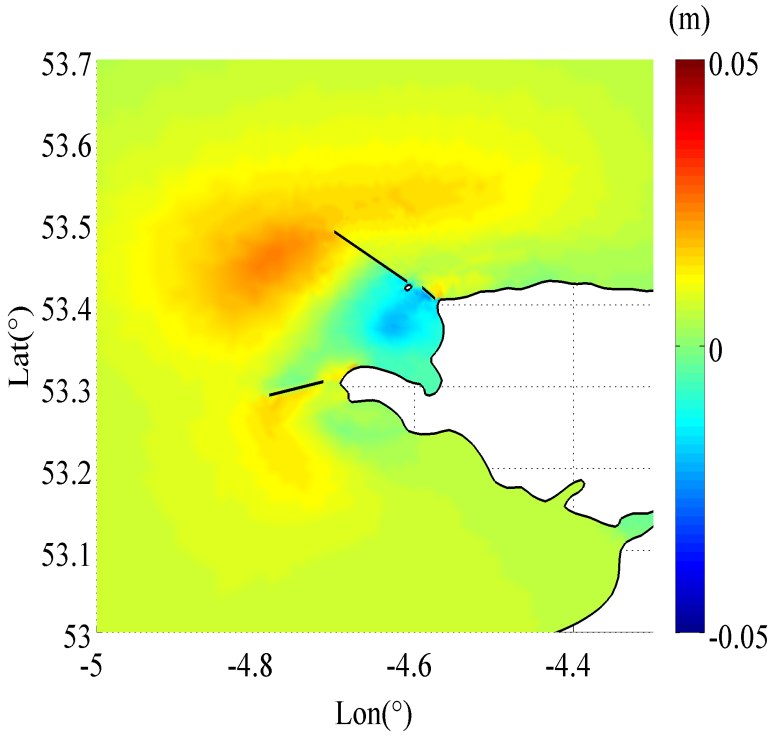

d) HH, SO and SS arrays

Figure 4 M_2 amplitude change from natural conditions off Anglesey due to the presence of different array configurations

Table 6 shows that significant changes occur in the M_2 current amplitudes in the vicinity of the arrays. The changes in the M_2 current amplitudes are calculated for each case study (and presented in Figure 5). Bearing in mind that the tides are bidirectional, reductions in the current amplitudes at both sides of the arrays are expected. For each case study, Figure 5 illustrates that the by-pass flow increases at the ends of the arrays. Due to the irregular bathymetry, the velocity magnitudes exhibit strong variations near the arrays.

Figure 5(a) shows that the presence of the HH + SO arrays cause the flow to divert both further offshore and towards the strait between Skerries and the Anglesey headland. Figure 5(b) illustrates the array configuration for HH and SS. It is seen that the flow is diverted primarily further offshore, increasing the M_2 velocity magnitude at the Anglesey Skerries site. Figure 5(c) shows that SO + SS increases the by-pass flow approximately by 0.5 m/s at the north end of the SO array. This increment decreases radially as the bathymetry of the site changes. The flow velocity is decreased more at the shallower ends of the arrays. Lastly, Figure 5(d) illustrates the M_2 velocity magnitude change for when all the arrays are operating together. The presence of HH array in this configuration contributes negatively as it enhances the flow diversion before the flow reaches the SO + SS arrays. However, as the arrays are far away from each other, the disturbance to the flow caused by HH array is relatively small.

The analyses conducted in this section confirm that the presence of tidal array in a partially blocked flow enhances the bypass flow.

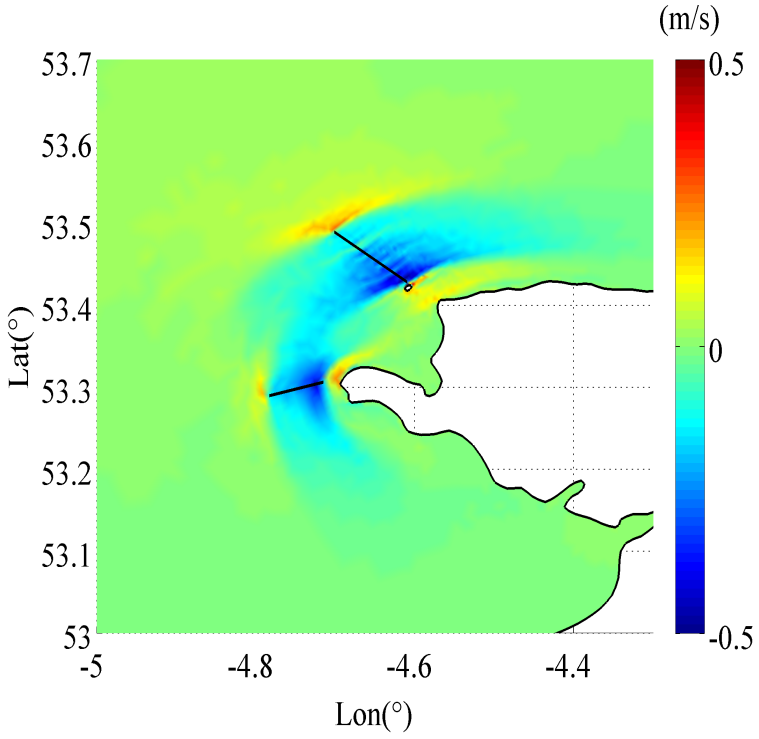

a) HH and SO arrays

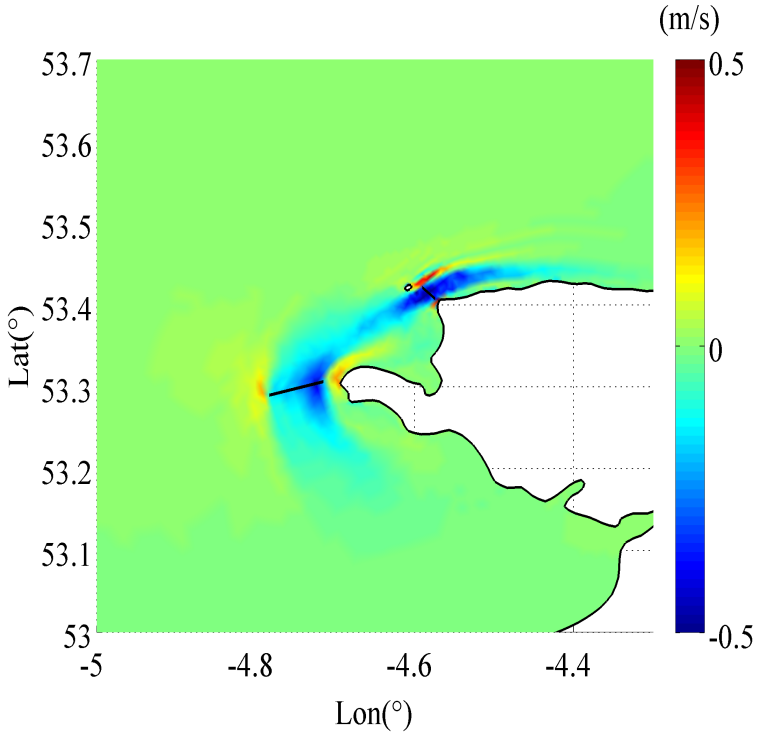

b) HH and SS arrays

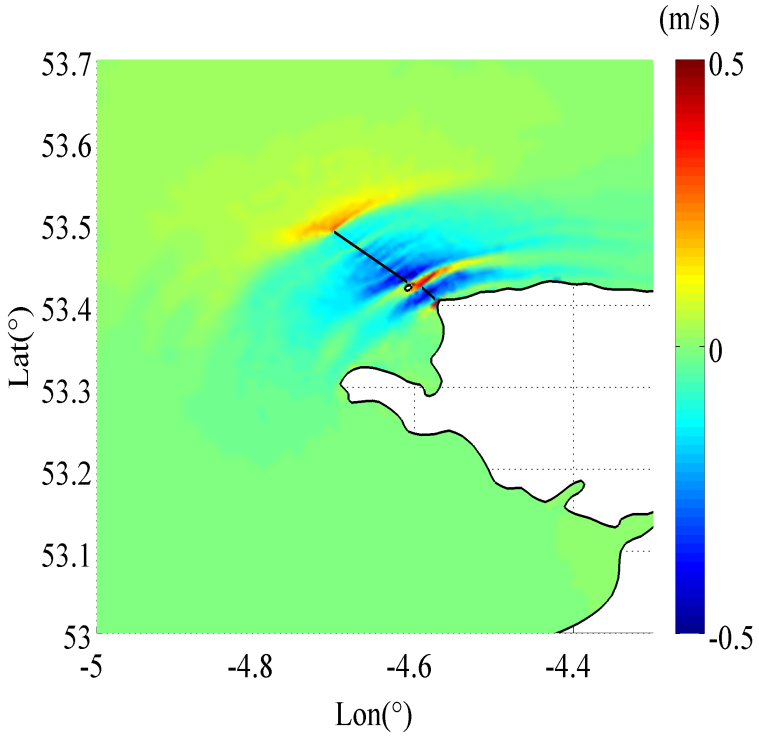

c) SO and SS arrays

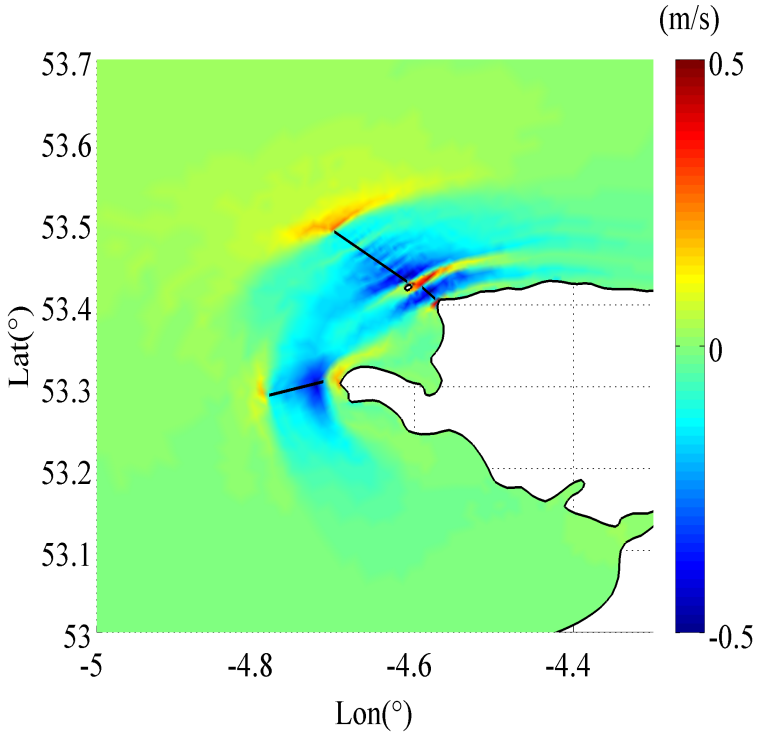

d) HH, SO and SS arrays

Figure 5 M_2 current speed change from natural conditions off Anglesey due to the presence of different array configurations

3. Bristol Channel

Description of the Model

Following the same methodology as described in Section 2, Figure 6 illustrates the map of the undisturbed kinetic energy flux density off the Bristol Channel site. It can be seen that there are several locations in this site, which are favourable for tidal array deployments. The sites that are chosen for analysing the tidal farm interactions are summarised in Table 11.

The analysis follows the same approach as taken in WG3 WP6 D7. Here, it is intended to examine the extent of the disturbance to the local hydrodynamics caused by the presence of the turbine arrays. In each simulation, the effect of the turbine array is represented using linear momentum actuator disk theory for a high blockage ratio ($B = 0.5$) and the computed optimum wake velocity coefficient. Each simulation covers a full spring-neap cycle. The forcing harmonics are the dominant semidiurnal M_2 and S_2 tides. The model parameters include the Coriolis force and a constant eddy viscosity term of 3 kg/(s.m). The bed friction coefficient used in the simulations is $C_f = 0.0025$.

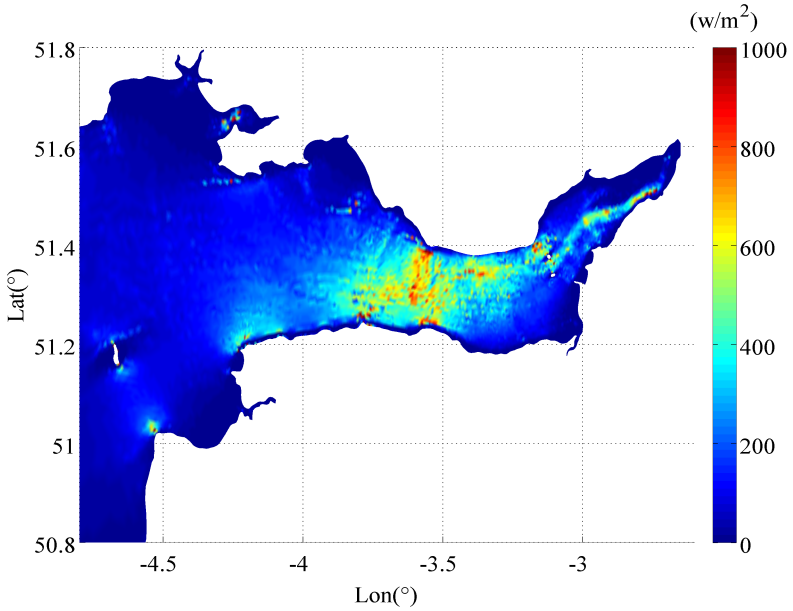

Figure 6 Undisturbed kinetic energy density map - the Bristol Channel

Site	Location	Coordinates	Undisturbed kinetic energy flux density, ρ_{KE} (W/m^2)
Bristol Channel	Lundy (LU)	51°5'26"N 4°35'79"W	175
	Ilfracombe (IL)	51°14'43"N 4°14'42"W	300
	Channel (BC)	51°17'46"N 3°30'10"W	500

Table 11 Locations where high tidal currents are observed at the Bristol Channel.

Analyses on Individual Array Deployments

This section presents a similar analysis as conducted in the Anglesey site. Firstly, the effect of individual arrays located around the Bristol Channel is investigated. The chosen sites around the Bristol Channel region are illustrated in Figure 7. These sites are examples of,

1. Lundy Array: Flow passing between an island and a headland,
2. Ilfracombe Array: Flow passing a headland and,
3. Channel Array: Flow in an oscillating bay.

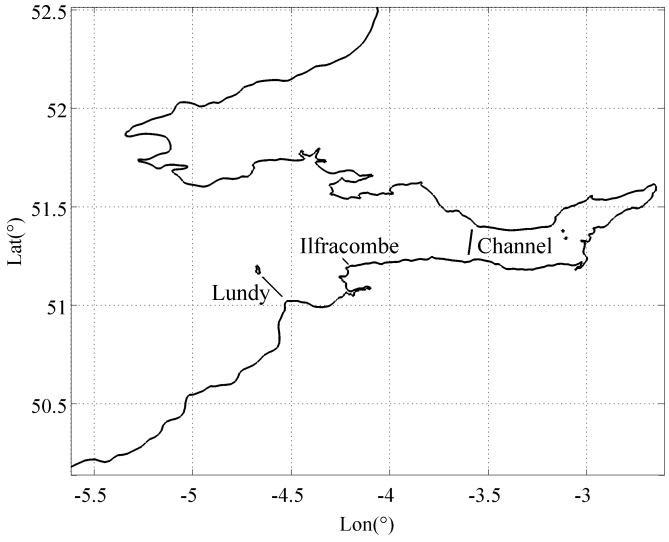

Figure 7 Locations of selected arrays in the Bristol Channel

A set of simulations is prepared for each array in order to determine the optimum wake velocity coefficients (α_4) that maximises the available power. The simulations consider a fixed blockage ratio (B = 0.5) while the α_4 values are varied. The model is forced with the dominant semi-diurnal tidal constituents M_2 and S_2. The time-varying power output is averaged over a spring-neap cycle. The averaged available power values are then fitted with a spline to calculate the maximum available power (Adcock *et al.*, 2013). The optimum wake velocity coefficients and corresponding maximum available power values are presented in Table 12.

Location	Length (km)	Optimum α_4	Maximum available power (MW)	Maximum extracted power (MW)
Lundy (LU)	13.2	0.40	162.7	315
Ilfracombe (IL)	4	0.47	47.8	80.4
Channel (CH)	14.4	0.40	311.6	604.7

Table 12 Optimum wake velocity coefficients for the arrays located at selected sites in the Bristol Channel. The maximum available and extracted power values are also given.

In order to evaluate the change in the tidal system, several comparison stations are chosen. These stations are distributed around the Celtic Sea from the outer Channel area to inner Channel (see Figure 8).

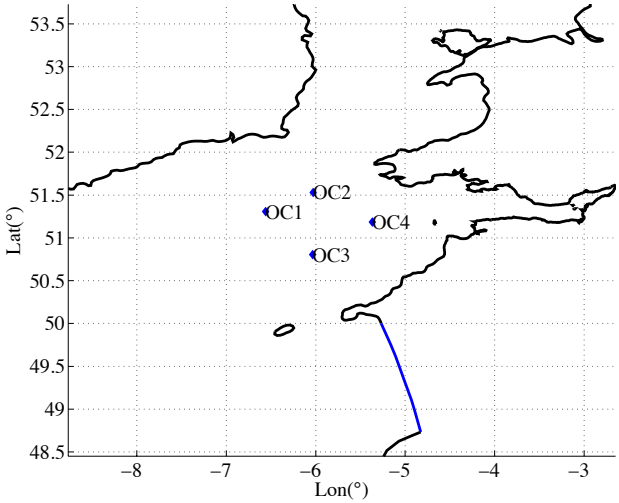

a) Outher Channel

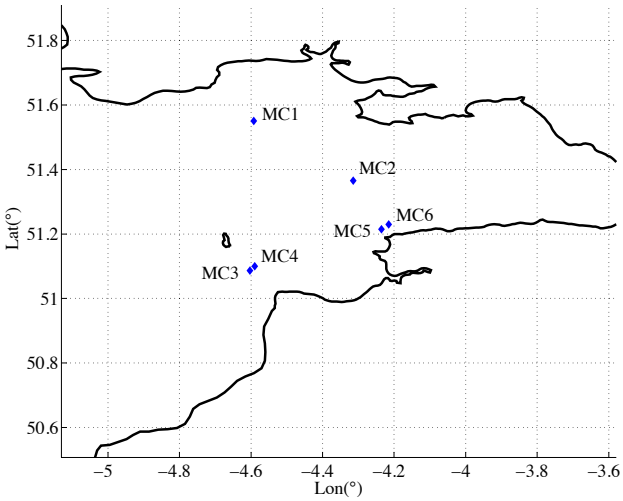

b) Mid-Channel

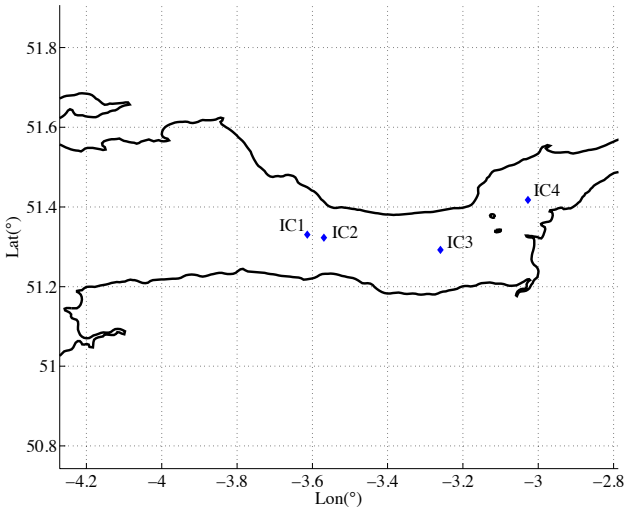

c) Inner Channel

Figure 8 Locations of stations around Bristol Channel chosen for purposes of comparison

As explained in WG3 WP6 D7, the Bristol Channel system is well known for its resonance characteristics. In WG3 WP6 D7, it was concluded that the resonance plays in important part in the available power output. The purpose of this section is to understand how the system responds in the case of deployment of arrays at different sites in the Bristol Channel.

Table 13 and Table 14 present the M_2 and S_2 tidal elevation amplitudes and phase lags computed at the stations in case of natural conditions (no tidal array deployments) and in cases of arrays installed at different sites. The results show that

M_2 and S_2 tidal elevation amplitudes are not affected significantly when arrays located on Lundy (LU) or Ilfracombe (IL) operate.

The deployment of Channel (CH) array, however, causes a reduction in the semi-diurnal M_2 and S_2 tidal elevations. The observed change in the outer Channel (Figure 8.a) and mid-Channel regions (Figure 8.b) are the M_2 tides are decreased by approximately 3 to 5 cm (Table 13). The CH array is located at the inner Channel and the results show that across the array, the M_2 tidal elevations are decreased by 8 cm. At the downstream of the array towards the Severn Estuary, the M_2 elevations are reduced by approximately 10 cm. Similarly, Table 14 shows that the S_2 tidal elevations are reduced by 5 cm throughout the Severn Estuary when the CH array is operating.

Station	Amplitude (m)				Phase (°)			
	Natural	*LU*	*IL*	*CH*	*Natural*	*LU*	*IL*	*CH*
OC1	1.61	1.60	1.61	1.58	155	155	155	155
OC2	1.62	1.62	1.62	1.59	165	165	165	165
OC3	1.91	1.91	1.91	1.89	150	150	150	150
OC4	2.14	2.13	2.14	2.11	162	162	162	162
MC1	2.72	2.71	2.72	2.68	173	174	173	173
MC2	2.92	2.91	2.92	2.87	171	171	171	171
MC3	2.64	2.65	2.64	2.61	162	161	162	162
MC4	2.65	2.65	2.65	2.62	163	164	162	163
MC5	2.96	2.95	2.96	2.92	166	167	166	167
MC6	2.99	2.98	2.99	2.95	167	168	168	167
IC1	3.64	3.63	3.64	3.56	180	181	181	180
IC2	3.66	3.65	3.67	3.58	181	181	181	184
IC3	4.08	4.08	4.09	3.98	187	187	187	189
IC4	4.40	4.41	4.43	4.31	192	193	193	194

Table 13 Amplitude and phase of the M_2 tidal elevations at observation stations in the Bristol Channel and Celtic Sea under natural conditions and in the presence of different array configurations.

The M_2 phase lags (Table 13) indicate insignificant changes while either Lundy (LU) or Ilfracombe (IL) arrays are operating. The maximum phase difference is observed when Channel (CH) array is operating. However, the change in the phase lag is only 3°, which implies that high tides are delayed by approximately 6 min

immediately east of the array.

Station	Amplitude (m)				Phase (°)			
	Natural	*LU*	*IL*	*CH*	*Natural*	*LU*	*IL*	*CH*
OC1	0.51	0.51	0.51	0.51	205	204	205	204
OC2	0.54	0.54	0.54	0.54	216	216	216	216
OC3	0.62	0.63	0.63	0.62	198	198	198	197
OC4	0.71	0.72	0.72	0.71	211	211	211	211
MC1	0.89	0.89	0.90	0.89	222	223	222	222
MC2	0.95	0.95	0.95	0.94	220	221	221	220
MC3	0.88	0.89	0.88	0.87	211	210	211	210
MC4	0.88	0.87	0.88	0.88	211	213	211	211
MC5	0.97	0.96	0.97	0.96	216	217	216	216
MC6	0.97	0.97	0.97	0.97	217	218	218	217
IC1	1.10	1.09	1.10	1.08	234	235	235	233
IC2	1.11	1.10	1.10	1.05	235	236	236	239
IC3	1.18	1.18	1.19	1.13	244	245	245	247
IC4	1.24	1.24	1.25	1.19	252	253	253	255

Table 14 Amplitude and phase of the S_2 tidal elevations at observation stations in the Bristol Channel and Celtic Sea under natural conditions and in the presence of different array configurations.

Table 14 shows that the Celtic Sea – Bristol Channel system behaves in a similar manner regarding the S_2 tidal phase lags. The high tides are delayed by 8 min east of the Channel (CH) array. However, there are no significant effects observed in the presence of LU and IL arrays.

The change in the currents is presented by focusing on M_2 and S_2 tidal constituents. Table 15 shows the M_2 magnitude and phase lags computed at the observation stations for natural case study as well as in the presence of the arrays. M_2 current characteristics (eccentricity and inclination) are presented in Table 16.

Table 15 indicates that the Lundy (LU) array causes a slight reduction in the M_2 velocity magnitudes at stations OC1 and OC3 but a small increment at stations OC2 and OC4. The stations just before and after the LU array show that, due to the energy extraction, the M_2 velocity magnitudes are decreased by approximately 4%. The array wake extends towards the MC5 and MC6 stations where there is 1% reduction in the M_2 velocity magnitudes. The inner Channel (Severn Estuary) site is not affected

greatly due to the presence of LU array. The M_2 phase lags are similar to that of the natural case for the outer stations when LU is operating. However, when the current reaches the LU array, MC3 and MC4 station readings show that the maximum velocities are observed approximately 15 min earlier than natural. The stations located far east of the LU array indicate that the maximum velocities are observed at similar times to that of the natural case.

Operating the Ilfracombe (IL) array causes minor changes in M_2 velocity magnitudes until the flow reaches the array. Stations at the upstream and downstream of the IL array (MC5 and MC6) show that the M_2 velocity magnitudes are reduced by 11%. The stations located at the inner Channel region show that the velocity magnitudes are slightly increased when compared to the naturally occurring velocities. The M_2 phase lags indicate that the maximum currents are observed 12-14 min earlier than the natural case at stations MC5 and MC6 that are located right before and after the IL array. However, there is no other change observed at other stations by means of the times when fast currents occur.

Station	U_{mag} (m/s)				φ_{mag} (°)			
	Natural	*LU*	*IL*	*CH*	*Natural*	*LU*	*IL*	*CH*
OC1	0.3118	0.3108	0.3110	0.3147	153	153	153	155
OC2	0.4950	0.4967	0.4968	0.5033	202	203	203	202
OC3	0.3781	0.3762	0.3770	0.3734	114	114	114	115
OC4	0.4994	0.5008	0.4993	0.4920	90	90	90	90
MC1	0.5976	0.5999	0.6010	0.5805	83	85	84	83
MC2	0.8703	0.8690	0.8791	0.8385	94	94	95	95
MC3	0.8401	0.8086	0.8389	0.8185	101	93	101	102
MC4	0.8434	0.8056	0.8431	0.8221	101	93	101	102
MC5	1.2418	1.2291	1.0968	1.2258	90	89	84	90
MC6	1.1469	1.1395	1.0120	1.1255	92	91	85	93
IC1	1.4932	1.4960	1.5004	1.3353	282	282	282	281
IC2	1.4366	1.4378	1.4420	1.2946	282	282	282	281
IC3	1.1471	1.1438	1.1472	1.1008	103	103	103	104
IC4	1.1518	1.1551	1.1589	1.1111	114	114	114	115

Table 15 Amplitude and phase of the M_2 tidal current at different observation stations in the Bristol Channel and Celtic Sea, under natural conditions and in presence of different array configuration.

Comparing the results obtained when the Channel (CH) array is operating to the naturally occurring M_2 tidal currents, it is seen that the system responds differently to the previous arrays discussed. This is believed to be mainly due to the fact that CH array is altering the resonance effects observed in the Bristol Channel. Overall, it is observed that apart from the stations OC1 and OC2, the M_2 velocity magnitudes recorded at the other stations all decrease. Bearing in mind that the M_2 elevations also decrease at the Severn Estuary when CH array is operating, it seems evident that the system is moving away from resonant frequency. The reduction in the M_2 velocity magnitudes is approximately 10% at the upstream and downstream of the array (station IC1 and IC2). The maximum M_2 currents are observed at the same time periods when compared to the undisturbed flow conditions. Although, there is a significant impact on the response of the Bristol Channel system by operating the CH array, this does not affect the timing of the fastest currents.

Station	Eccentricity				Inclination (°)			
	Natural	*LU*	*IL*	*CH*	*Natural*	*LU*	*IL*	*CH*
OC1	0.3461	0.3457	0.3462	0.3332	40	40	40	41
OC2	0.2934	0.2917	0.2918	0.2805	80	80	80	80
OC3	0.2333	0.2357	0.2338	0.2429	34	34	34	35
OC4	0.5635	0.5732	0.5631	0.5871	6	6	6	6
MC1	0.0901	0.0787	0.0884	0.0924	14	15	15	15
MC2	0.0613	0.0458	0.0586	0.0636	12	12	12	12
MC3	0.0943	0.0826	0.0950	0.0965	33	33	34	34
MC4	0.0956	0.0774	0.0965	0.0970	33	33	34	34
MC5	0.0137	0.0075	-0.0205	0.0073	31	31	31	32
MC6	0.0124	0.0074	0.0140	0.0138	23	22	22	24
IC1	0.0108	0.0114	0.0112	0.0278	174	174	174	175
IC2	0.0111	0.0118	0.0115	0.0200	173	173	173	173
IC3	-0.0151	-0.0147	-0.0146	-0.0134	8	8	8	8
IC4	0.0388	0.0373	0.0374	0.0360	59	59	59	59

Table 16 Eccentricity and inclination of the M_2 tidal current at different observation stations in the Bristol Channel and Celtic Sea, under natural conditions and in presence of different array configurations.

Table 16 shows the M_2 current ellipse parameters at the observation stations for different cases. From the table, it is seen that installing the LU array alters the ellipse

structure very mildly at the Celtic Sea front. The eccentricity is decreased at the stations located in the mid-Channel region. The flow is still rectilinear. When the IL array is in operation, the system responds in a similar manner as in described for the LU array. The eccentricity is changing significantly at MC5, which is located at the upstream of the array (regarding the direction of the flood tide), which indicates that the M_2 ellipse is changing direction from anti-clockwise to clockwise. When the CH array is in operation, the change in the eccentricity varies throughout the Celtic Sea – Bristol Channel system. There is a slight decrease in eccentricity observed at the outer Channel stations OC1 and OC2, whereas it tends to increase slightly until the flow reaches the Ilfracombe headland. The eccentricity is doubled at the inner Channel stations IC1 and IC2, which are located at the upstream and downstream of the array. Bearing in mind that the tidal devices do not exert a force in the tangential direction, the semi-minor velocities are not affected by the energy extraction. This, in turn, translates into an increment in the eccentricities as the semi-major axis values are decreased.

Station	U_{mag} (m/s)				φ_{mag} (°)			
	Natural	*LU*	*IL*	*CH*	*Natural*	*LU*	*IL*	*CH*
OC1	0.1416	0.1396	0.1399	0.1394	188	187	187	188
OC2	0.1761	0.1729	0.1732	0.1739	229	230	230	229
OC3	0.1545	0.1540	0.1543	0.1529	162	161	161	161
OC4	0.1771	0.1781	0.1772	0.1746	151	152	151	151
MC1	0.1780	0.1768	0.1782	0.1708	136	140	138	136
MC2	0.2750	0.2732	0.2785	0.2617	149	150	151	150
MC3	0.2967	0.2878	0.2963	0.2887	154	142	154	154
MC4	0.2960	0.2847	0.2956	0.2877	154	143	154	155
MC5	0.4095	0.4034	0.3400	0.4014	138	138	132	138
MC6	0.3734	0.3674	0.3036	0.3636	140	141	133	142
IC1	0.4507	0.4513	0.4533	0.3896	338	339	339	339
IC2	0.4368	0.4352	0.4373	0.3676	338	339	339	340
IC3	0.3265	0.3229	0.3243	0.3056	162	163	162	164
IC4	0.3432	0.3426	0.3438	0.3274	173	175	175	176

Table 17 Amplitude and phase of the S_2 tidal current at different observation stations in the Bristol Channel and Celtic Sea, under natural conditions and in presence of different array configuration.

Table 17 and Table 18 present the S_2 tidal current characteristics of: magnitude, phase lag, eccentricity and inclination. Table 17 shows that operating tidal arrays cause a small reduction in the S_2 velocity magnitudes at the outer Channel stations. Similarly to M_2 tidal current analysis, S_2 velocity magnitudes are decreased at the observation stations that are placed in the vicinity of the arrays. The maximum change in the velocity magnitudes is observed when the Ilfracombe (IL) array is operating. The S_2 velocity magnitudes are reduced by approximately 18%. This is mainly due to the fact that the flow is partially blocked, which forces it to divert around the edges of the array and, also reduces the mass flux passing through the array. Operating the Channel (CH) array reduces the S_2 velocity magnitudes across the Celtic Sea and Bristol Channel area. The maximum reduction is approximately 15%, which is observed at the stations located at the upstream and downstream of the array. The S_2 velocity phase lags changes are similar to the M_2 phase changes. The maximum S_2 tidal currents are observed approximately 20 min earlier than the natural case when Lundy (LU) array is operating. As far as the Ilfracombe (IL) array is concerned, the maximum S_2 currents occur 12 min prior to the natural case. The effect of Channel (CH) array to the S_2 phase lags is insignificant.

Table 18 presents the characteristic parameters of S_2 tidal currents. Table 18 shows that the effect of deployment of arrays seen at the outer Channel site is small when the S_2 tidal current ellipse structure is concerned. When the LU array is operating, the eccentricity of S_2 currents decreases at the stations in the vicinity of the array location, as well as the stations located in the Severn Estuary. This implies that the semi-minor axis values are also decreasing. The ellipse size is reduced throughout the Bristol Channel area. Similarly, the eccentricity decreases within the Bristol Channel site when Ilfracombe (IL) array is operating. As discussed earlier on M_2 current analysis, the eccentricity of S_2 current ellipses increase when Chanel array (CH) is in operation.

In terms of change in inclination, the operation of arrays shows no significant change to this parameter. This implies that the angle between the semi-major axis relative to the horizontal velocity axis does not change due to the energy extraction.

Station	Eccentricity				Inclination (°)			
	Natural	*LU*	*IL*	*CH*	*Natural*	*LU*	*IL*	*CH*
OC1	0.2014	0.2020	0.2023	0.2009	35	34	34	35
OC2	0.3488	0.3553	0.3561	0.3457	71	71	71	71
OC3	0.1579	0.1567	0.1549	0.1585	36	36	36	37
OC4	0.5321	0.5412	0.5296	0.5442	23	24	23	24
MC1	0.0897	0.0771	0.0983	0.1062	18	19	18	19
MC2	0.0298	-0.0015	0.0237	0.0316	15	14	15	15
MC3	0.0739	0.0632	0.0832	0.0831	35	35	36	36
MC4	0.0798	0.0777	0.0881	0.0867	36	35	36	36
MC5	-0.0294	-0.0304	-0.0400	-0.0087	31	31	32	32
MC6	-0.0174	-0.0205	-00075	-0.0012	23	23	23	24
IC1	0.0184	0.0067	0.0058	0.0413	175	175	175	175
IC2	0.0143	0.0028	0.0028	0.0383	174	173	173	173
IC3	0.0292	0.0257	0.0267	0.0306	8	8	8	8
IC4	0.0276	0.0213	0.0225	0.0194	59	59	59	60

Table 18 Eccentricity and inclination of the S_2 tidal current at different observation stations in the Bristol Channel and Celtic Sea, under natural conditions and in presence of different array configurations.

Analyses of Multiple Array Deployments

This subsection considers the effect of installing multiple arrays within the Bristol Channel site. The array configurations studied in this section are:

1. Lundy and Ilfracombe (LU + IL),
2. Lundy and Channel (LU + CH),
3. Ilfracombe and Channel (IL + CH) and,
4. Lundy, Ilfracombe and Channel (LU + IL + CH).

The simulations are designed by operating each array using the optimum wake velocity coefficients presented in Table 12. Table 19 compares the maximum available power outputs that are averaged over a spring tide for each case study with the arithmetic sum of the individual maximum power available to the arrays in isolation. From Table 19, it is seen that the Lundy (LU) and Ilfracombe (LU) arrays are not interacting with each other significantly in terms of available power (see Table 19- Case Study 1).

However, operating the Channel (CH) array in combination with other arrays,

improves the performance of the CH array. This unexpected result (given that the CH array is in series with the other sites) is mainly due to the slight rise in the head at the upstream of the CH array caused by operation of other arrays. As the mass flux passing through the CH array is increased, the available power to that array is increased as well.

Case Study	Array Combinations	P_{avail} (MW)	$\sum P_{avail}$ (MW)
1	LU + IL	213.6	210.5
2	LU + CH	503.9	474.3
3	IL + CH	391.3	359.4
4	LU + IL + CH	546.7	522.1

Table 19 Comparison of the estimated (P_{avail}) and calculated (ΣP_{avail}) available power output for each test case studied for Bristol Channel region.

The change in the flow field is evaluated by focusing on the M_2 tidal elevations and M_2 tidal current magnitudes. Figure 9 shows the change in M_2 tidal elevations when multiple arrays are operating. Case 1 considers the deployment of Lundy and Ilfracombe arrays together. Figure 9(a) illustrates that the M_2 surface elevations are increased by 5 cm towards the Celtic Sea region. However, the elevations are decreased by an average of 1.5 cm at the Channel side of the basin. The rapid change in elevations observed in Swansea Bay is due to the wetting and drying treatment applied to the model, and is not considered to be significant.

In the previous subsection it was observed that operating the Channel array causes a change in M_2 elevations from Minehead towards the tip of the Bristol Channel. As the array is effectively decreasing the length of the Bristol Channel, the response of the system shifts away from the resonance frequency. This implies a reduction in observed water surface elevations. Operating Lundy array with the Channel array (Figure 9.b) also results in this reduction at the east of the Bristol Channel. However, this configuration causes a small increment (~1 cm) in M_2 elevations just in front of the Channel array. Figure 9(c) and Figure 9(d) show that the system responds in a

similar manner in case of other array configurations.

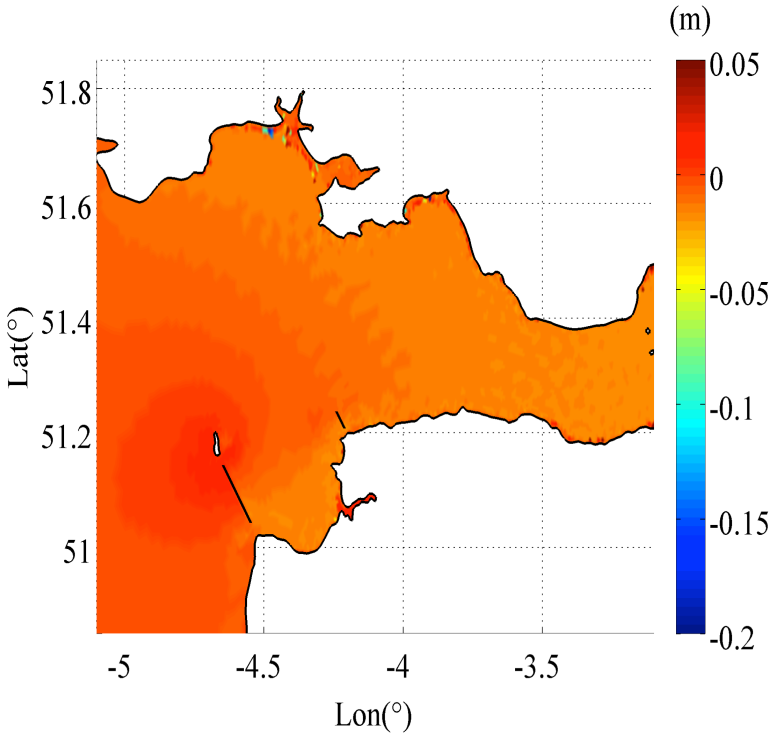

a) LU and IL arrays

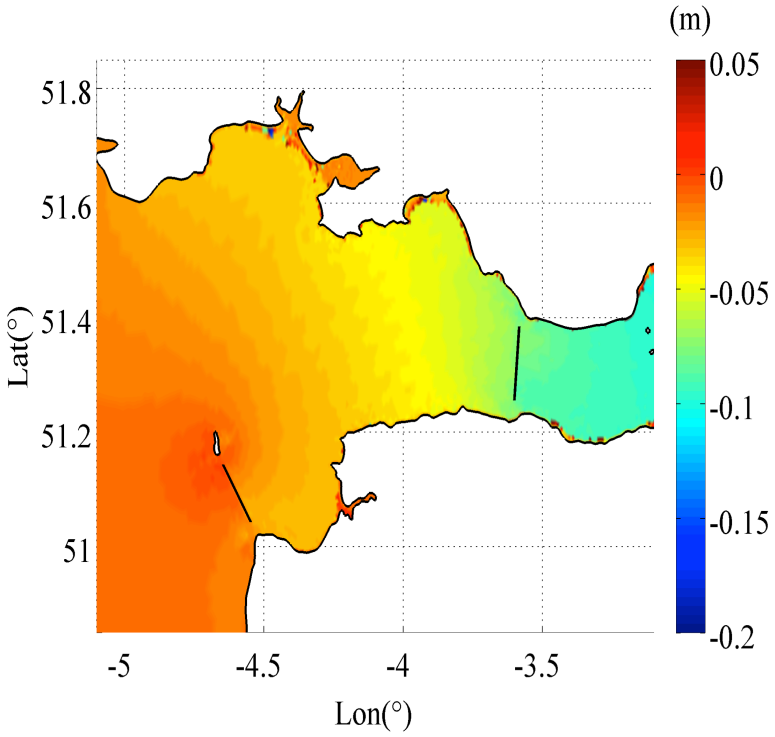

b) LU and CH arrays

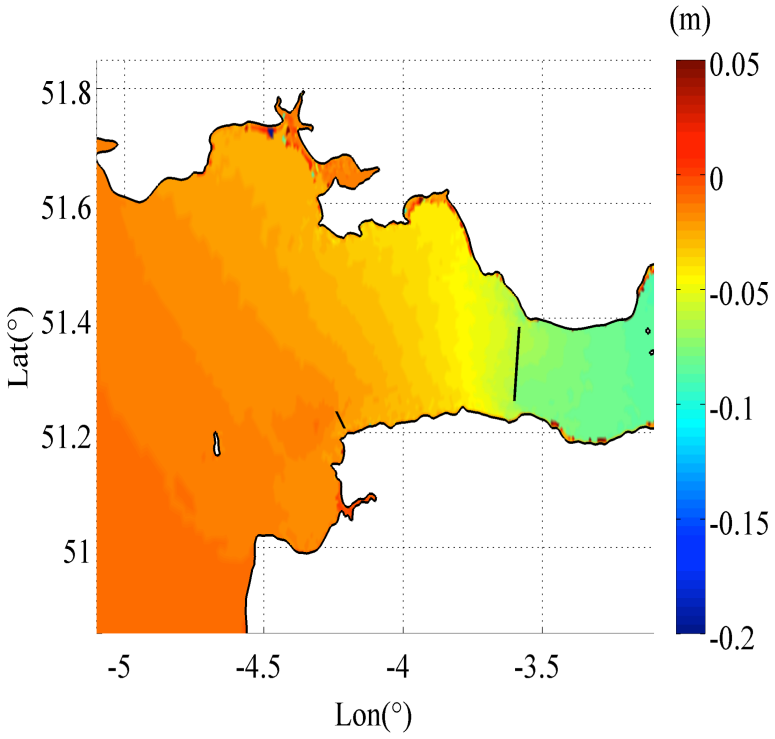

c) IL and CH arrays

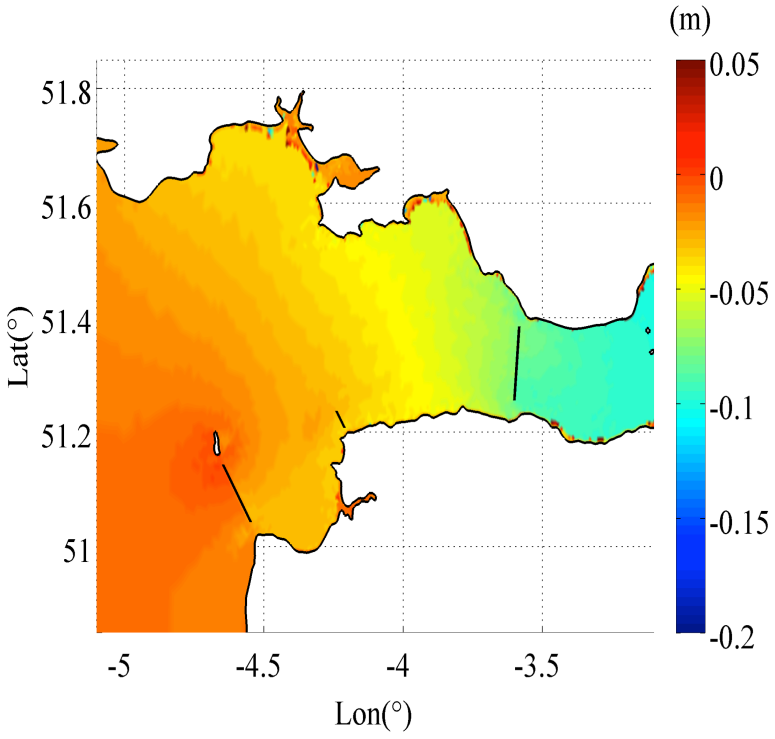

d) LU, IL and CH arrays

Figure 9 M_2 amplitude change in presence of different array configurations

Figure 10 plots the system response to the presence of different array configurations with respect to the M_2 tidal current changes. From the figure, it is seen that the flow accelerates at the edges of the arrays due to the thrust applied to the flow by the arrays. Figure 10(a) illustrates the combination of Lundy (LU) and Ilfracombe (IL) arrays. From this figure, it is seen that the flow is diverted to the north of Lundy Island as the LU array is operating. The presence of IL array also contributes into this diversion. Figure 10(b) shows the array configuration of Lundy (LU) and Channel (CH) arrays. From the figure, there is not a direct interaction between arrays by means of change in the M_2 current velocities. For both arrays, the by-pass flow is accelerated due to the thrust applied by the turbines. Figure 10(c) presents the results obtained for operating Ilfracombe (IL) array with the Channel (CH) array. Even though the arrays are closer to each other when compared to the array combination discussed in Figure 10(b), there is no evident hydrodynamic interaction observed. Figure 10(d) shows the change in M_2 velocity magnitudes when all three arrays are operating together. This figure also confirms that the by-pass flow is accelerated at the ends of the arrays, but there is no significant interaction between the arrays in terms of tidal hydrodynamics of the system.

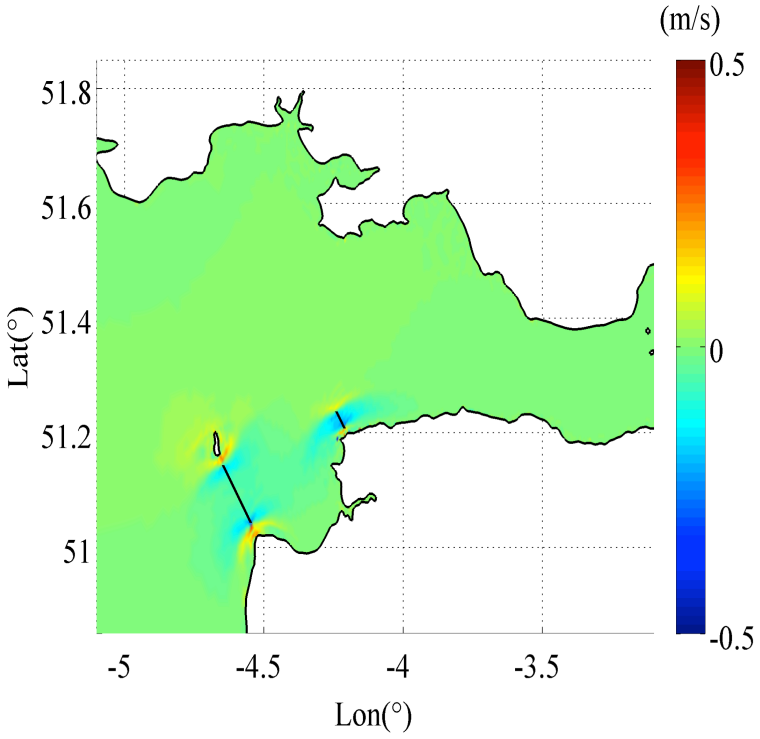

a) LU and IL arrays

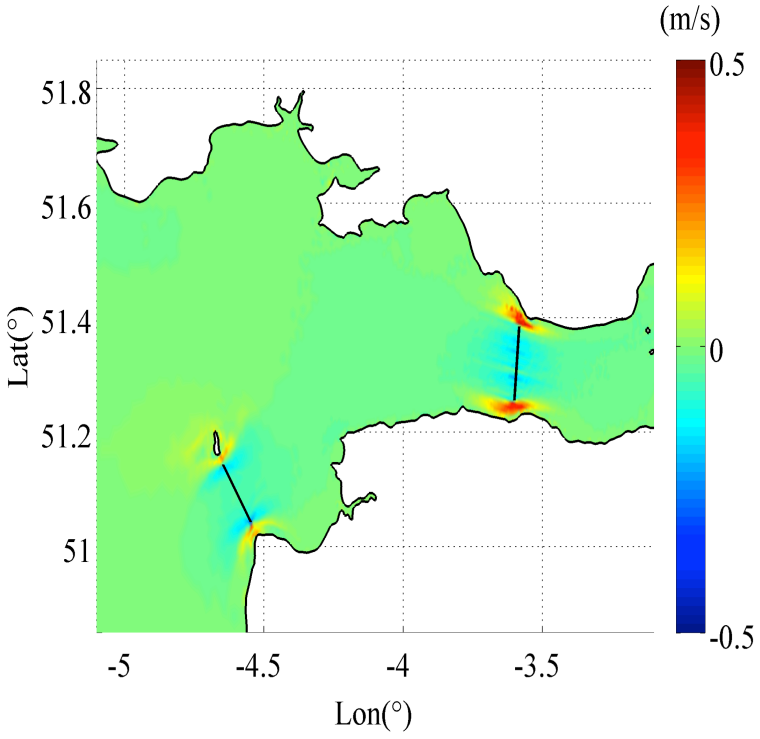

b) LU and CH arrays

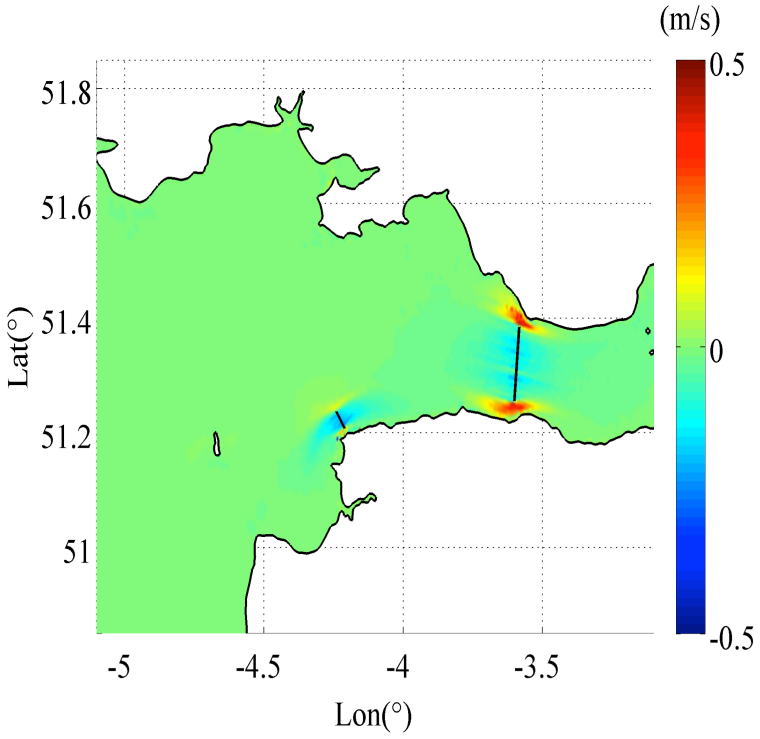

c) IL and CH arrays

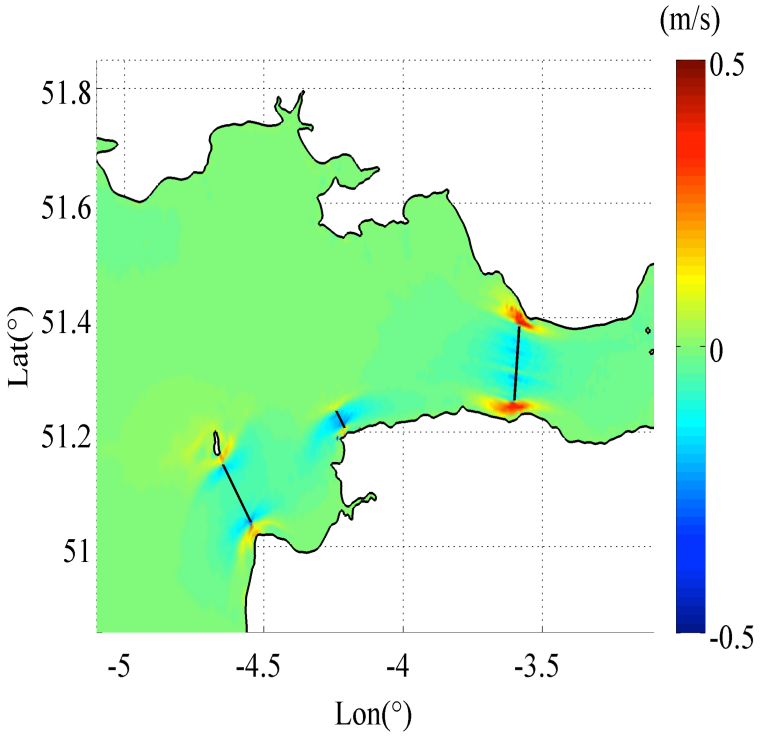

d) LU, IL and CH arrays

Figure 10 M_2 current change in presence of different array configurations

4. Anglesey and the Bristol Channel

Previous sections consider the analyses regarding the power available to the turbines and the hydrodynamic effect of extracting energy from the tidal stream off Anglesey and in the Bristol Channel. WG3 WP6 D4B explains that these sites are relatively close to each other, thus there may be hydrodynamic interactions in the case of operating tidal farms at both these sites.

In order to investigate longer distance interaction effects, an additional test case has been prepared which considers operating all of the 6 arrays together. The model parameters are the same as in the previous analyses. The arrays are defined by the computed optimum wake velocity coefficients. This test case also considers a high blockage ratio to be applied to the flow ($B = 0.5$). Table 20 summarises the arrays and the optimum wake velocity coefficients used in the simulation. Table 20 also shows the power available to the three arrays deployed at each of the main sites averaged over a spring-neap tidal cycle. Table 20 shows that the simulated total available power is trivially different from the sum of the three arrays operated at Anglesey and in the Bristol Channel independently: in other words the analysis indicates no significant long distance interaction between tidal farms.

Considering the change in the tidal dynamics of the system, the M_2 tidal elevations show a similar change when compared to the results presented in the previous sections. As for the M_2 currents (see Figure 11), the far-field velocities change approximately by 0.05 – 0.1 m/s. However, this change does not affect the sites directly. Thus, it is concluded that there is no significant hydrodynamic interaction between Anglesey and the Bristol Channel sites.

Array	Optimum α_4	Individual Array P_{avail} (MW)	Simulated P_{avail} (MW) for 3 arrays	$\sum P_{avail}$ (MW)	Simulated P_{avail} (MW)
Holyhead	0.48	168.3	668.4	1162.2	1212.9
Skerries-Offshore	0.46	385.8			
Skerries-Strait	0.55	86.0			
Lundy	0.40	162.7	546.7		
Ilfracombe	0.47	47.8			
Channel	0.40	311.6			

Table 20 Summary of the power available to the turbine arrays located off Anglesey and in the Bristol Channel.

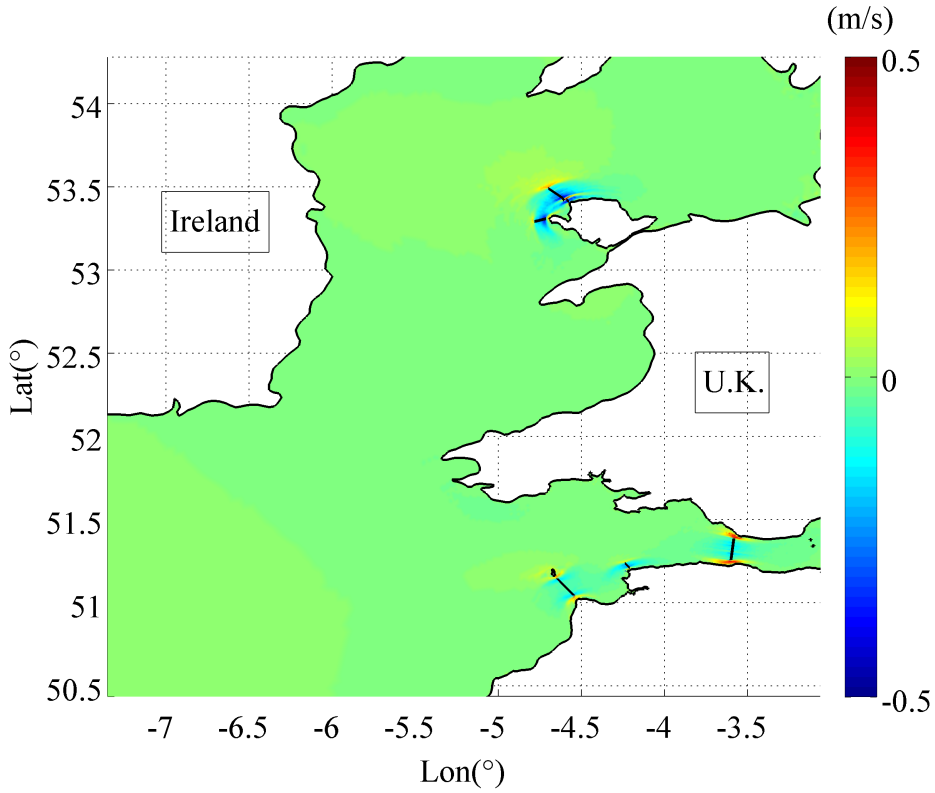

Figure 11 Change in the M_2 tidal current within the Irish Sea, Celtic Sea and the Bristol Channel in case of operating all arrays considered.

5. The Pentland Firth

The effects of deployment of tidal turbines in the Pentland Firth have been reported in three papers (see below), which cover this deliverable. They are included as appendices to this report and only a brief summary of the main conclusions is given below.

To extract significant power from the Pentland Firth will require a substantial change to the tidal dynamics within the Pentland Firth. This is simply shown by considering a point in the middle of the Firth and examining the change of current with different levels of energy extraction. Figure 12 shows this change in current for a point between the islands of Swona and Stroma.

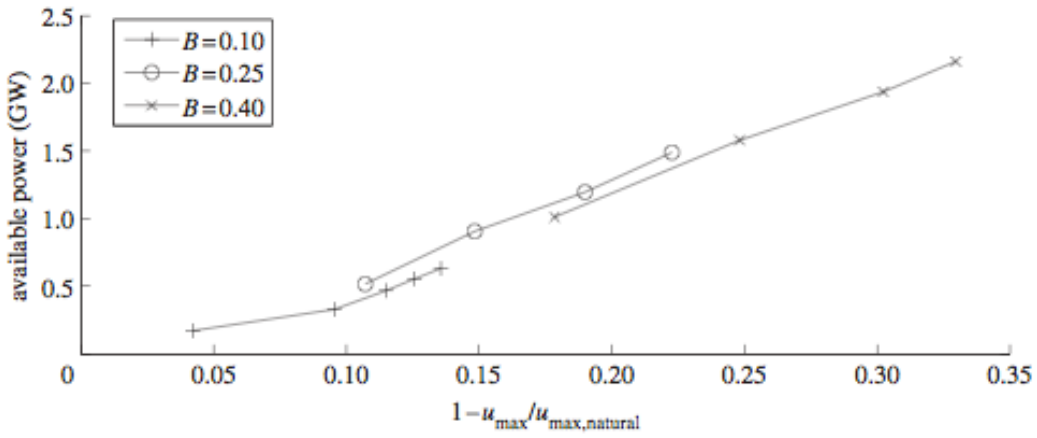

Figure 12 Change in the magnitude of the maximum current at location 58°43N-03°05W when tidal turbines are deployed to maximize time-averaged available power extraction. One to five rows are considered for B = 0.1. One to four rows are considered for B = 0.25 and B = 0.4. For further details see Adcock et al. (2013)

To examine the spatial changes in current in rather more detail let us consider the case with a blockage ratio of 0.4 and three rows of tidal turbines. This represents an extreme case and represents the highest level of energy extraction considered feasible in Adcock *et al.* (2013).

First consider the water levels across the domain. Figure 13 shows the change to the magnitude of the M_2 tidal amplitude in the vicinity of the Pentland Firth. The presence of tidal turbines causes small changes to the range of water levels within the Pentland Firth. However, outside the main channel the disturbance is negligible. The

S_2 tidal component shows a very similar response (not shown). The minimal disturbance outside the main channel implies that there will be minimal diversion of the flow around the north of the Orkney Islands.

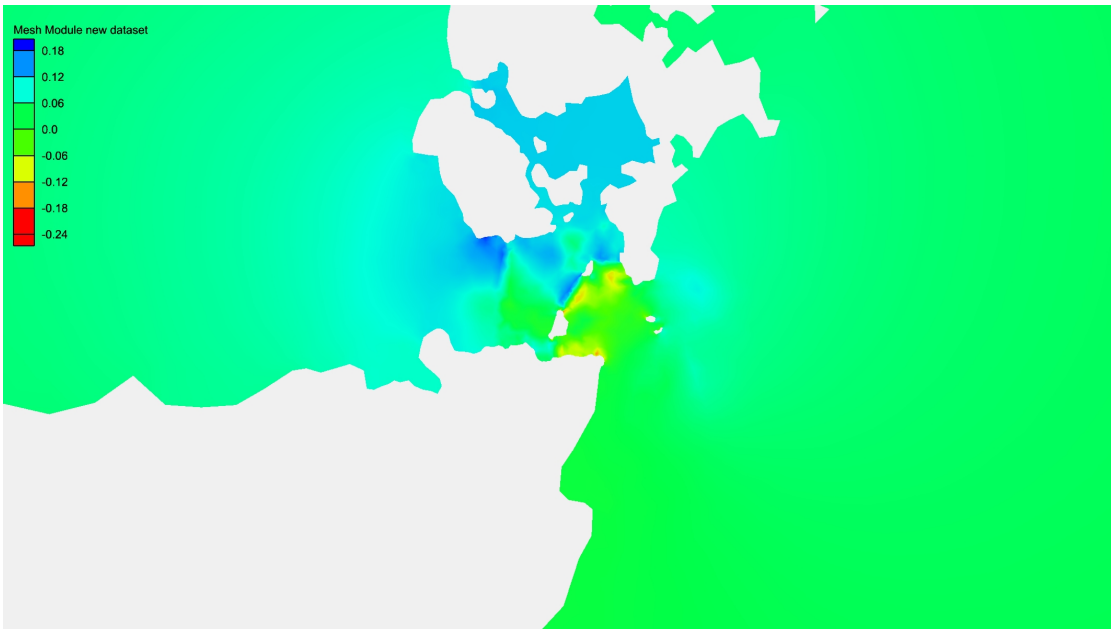

Figure 13 Change in M_2 water level when 3 rows of high blockage tidal turbines are deployed. Water level in m.

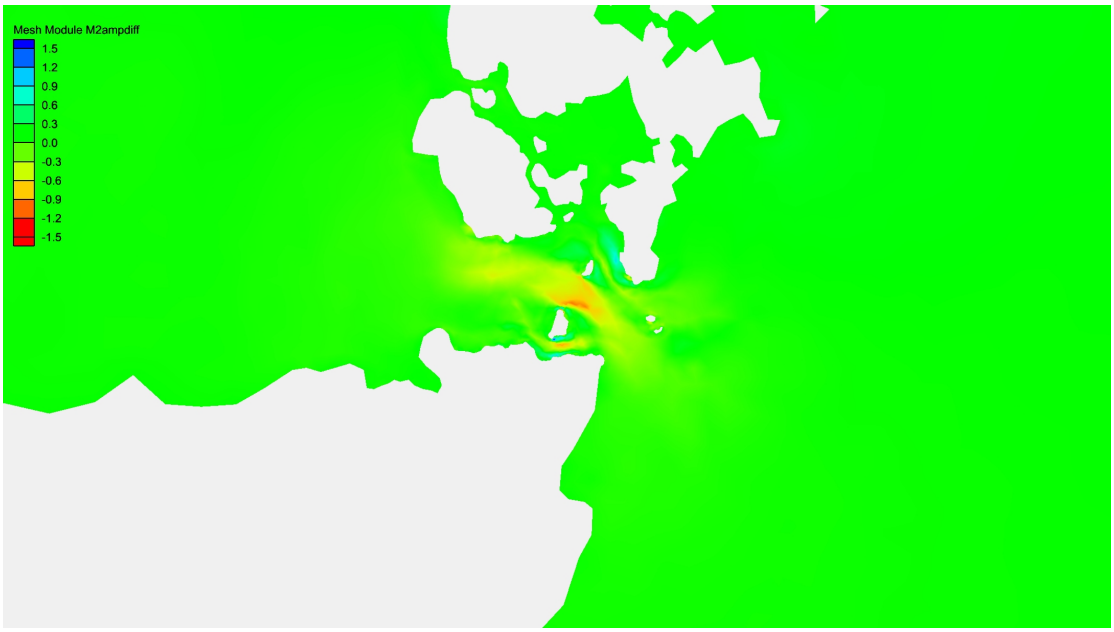

Figure 14 Change in M_2 velocity when 3 rows of high blockage tidal turbines are deployed. Speed in m/s.

We also can also examine the spatial change in velocity when a large number of tidal turbines (greater than 100 devices) are deployed. Figure 14 show the change in the M_2 velocity through the Pentland Firth when a large number of turbines are deployed.

As expected from Figure 12, there is a large difference in the flow through the central portion of the strait where the naturally occurring flow is greatest.

The environmental changes are also considered in three papers which have been produced as part of this deliverable and which have been accepted for publication. These are:

1. Adcock & Draper (2014) — This paper presents analysis of the magnitude of the different tidal harmonics for an idealised channel with energy extraction. The results are compared to the Pentland Firth model.

2. Draper *et al.* (2014a) — Analysis of the maximum energy extraction from different channels within the Pentland Firth and the change in current in those channels.

3. Draper *et al.* (2014b) — A theoretical explanation of how blocking different channels changes the current in parallel channels. The results of Draper *et al.* (2014a) are used as examples to validate the semi-analytical model.

6. Conclusions

This report examines the basin-scale environmental changes that occur when large arrays of tidal stream turbines are operating in a tidal basin. Three sites are analysed individually:

- Anglesey,
- The Bristol Channel and,
- The Pentland Firth.

Among these sites, Anglesey and the Bristol Channel are also analysed as a combined simulation to evaluate the possible hydrodynamic interaction between tidal energy farms.

Some common conclusions are drawn using the analysis conducted herein. The

presence of tidal turbines causes a reduction in the flow through the turbine array relative to the case wherein there were no turbines present. It is seen that, if the turbine array extend across an entire channel then the thrust applied to the flow speed may be reduced in the far-field as well as in the vicinity of the array. In the case of a partially blocked flow, there will be a fast bypass flow around the ends of the turbine array. However, the total flow passing through the turbine array is reduced due to the thrust applied by the array on the flow.

The changes to the tidal dynamics are geographically contained to the near vicinity of the turbine array. Hence, there is virtually no interaction between the turbine array between Anglesey and the Bristol Channel.

The greatest disturbance observed in this study occurs in the Bristol Channel. This is unsurprising as the Bristol Channel is well known to be a resonant system and so is much more sensitive to perturbation than other sites.

Overall, at peak available energy extraction, there would be a measureable change in the tidal dynamics, which might lead to a significant environmental impact, although assessing the impact itself is beyond the scope of this project. Taking these effects into account is of importance when designing a tidal turbine farm, as there may need to be a compromise between the change to the tidal dynamics and the amount of power to be generated.

REFERENCES

Adcock, T.A.A. and Draper, S. (2014) Power extraction from tidal channels — multiple tidal constituents, compound tides and overtides, accepted, *Renewable Energy*.

Adcock, T.A.A., Draper, S., Houlsby, G.T., Borthwick, A.G.L. and Serhadlıoğlu, S. (2013) The available power from tidal stream turbines in the Pentland Firth. *Proceedings of Royal Society A* 469(2157) 20130072.

Admiralty (1986) Tidal stream atlas Orkney and Shetlands, 4th edn. NP209. Taunton, UK: Hydrographic Office

Draper, S., Adcock, T.A.A., Houlsby, G.T. and Borthwick, A.G.L. (2014a) Estimate of the Extractable Pentland Firth Tidal Stream Power Resource, accepted *Renewable Energy*.

Draper, S., Adcock, T.A.A., Houlsby, G.T. & Borthwick, A.G.L. (2014b). An Electrical Analogy for the Pentland Firth Tidal Stream Power Resource, accepted, Proceedings of the Royal Society A.

Draper S, Houlsby G.T., Oldfield M.L.G., Borthwick A.G.L. (2010) Modelling

tidal energy extraction in a depth-averaged coastal domain. *IET Renew. Power Gener*. **4**, 545–554.

Garrett, C. and Cummins, P. 2005 The power potential of tidal currents. *Proceedings of Royal Society A* 461.

Houlsby, G.T., Draper, S. and Oldfield, M.L.G. (2008) Application of Linear Momentum Actuator Disk Theory to Open Channel Flow, Technical Report, Department of Engineering Science, University of Oxford, UK.

Kubatko, E. J., Bunya, S., Dawson, C. Westerink, J. J. and Mirabito, C. 2009 A performance comparison of continuous and discontinuous finite element shallow water models. *J. Sci. Comput*. **40** (1-3), 315–339

Kubatko, E. J., Westerink, J. J. and Dawson, C. 2006 hp Discontinuous Galerkin methods for advection dominated problems in shallow water flow. *Computer Methods in Applied Mechanics and Engineering* **196** (1-3), 437 – 451.